# X-Ray Attenuation in Silicon and Germanium in the Energy Range 25 to 50 keV

L. Gerward and G. Thuesen

Laboratory of Applied Physics III, Technical University of Denmark, Lyngby, Denmark

(Z. Naturforsch. **32 a**, 588–593 [1977]; received March 25, 1977)

The X-ray attenuation coefficients of silicon and germanium single crystals have been measured using an energy-dispersive method with particular emphasis on the energy range 25 to 50 keV. The experimental results are compared with theoretical calculations of the photoelectric absorption as well as the attenuation due to the Compton scattering and thermal diffuse scattering.

## 1. Introduction

The knowledge of accurate X-ray attenuation coefficients is important in many fields such as fluorescence analysis, crystallography and anomalous transmission in perfect crystals. Recently, it has been shown that a theory of the photoelectric absorption of X-rays, based on Hönl's [1] and other authors' treatment of generalized scattering factors and using screened non-relativistic hydrogen-like eigenfunctions, is in good agreement with experimental and other theoretical data in the photon energy range 5 to 25 keV [2, 3, 4]. This energy range is sufficient for most experiments in standard X-ray diffractometry. However, the new methods of energy-dispersive diffractometry and the use of synchrotron radiation in the X-ray range make it important to know X-ray attenuation coefficients also for higher energies.

The present work describes a determination of the X-ray attenuation coefficients of silicon and germanium with particular emphasis on the energy range 25 to 50 keV. An energy-dispersive method using a continuous X-ray spectrum has been developed for the measurements. An advantage of the method is that the fundamental reflexion and the higher harmonics from the monochromator crystal are recorded separately in a multichannel analyser. In this way we have measured the attenuation coefficients for several energies in each experiment.

The experimental results are compared with calculations of the photoelectric absorption using hydrogen-like eigenfunctions and with more rigorous calculations based on relativistic quantum theory. The energy range was also chosen in order to study the additional attenuation processes, namely the thermal diffuse scattering and Compton scattering, in more detail.

Reprint requests to Dr. L. Gerward, Laboratory of Applied Physics III, Building 307, Technical University of Denmark, *DK-2800 Lyngby, Denmark*.

## 2. Experimental Arrangement

The experimental arrangement is shown in Figure 1. A continuous spectrum of X-rays was provided by a tungsten tube operated at 50 kV in a high-stabilized X-ray generator. The collimated beam was made monochromatic by diffraction in a silicon single crystal, cut parallel to the (111) planes. The energy spectrum of the X-ray photons scattered through a fixed angle, $2\theta_0$, was measured by a semiconductor detector connected to a multichannel pulse-height analyser. A Soller slit in front of the detector served to minimize undesired scattered radiation.

The absorbing samples are slices cut from dislocation-free single crystals. The silicon slices are cut parallel to the (100) planes in the thickness range 0.15 to 15 mm. The germanium slices are parallel to the (111) planes and 0.15 to 0.35 mm thick. During the measurement the absorber was placed perpendicular to the X-ray beam between the X-ray source and the monochromator.

Two kinds of semiconductor detectors were used: An Ortec Series 7000 Si(Li) detector and a Prince-

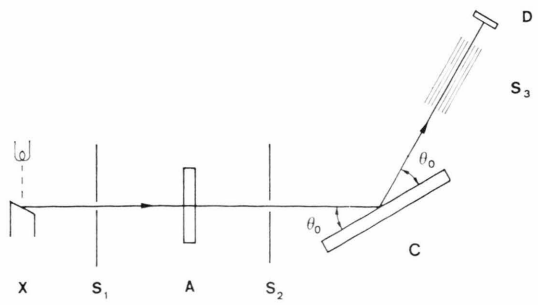


Fig. 1. Experimental arrangement. X = X-ray tube, $S_1$, $S_2$ = vertical slits, A = absorber, C = diffracting crystal, $2\theta_0$ = scattering angle, $S_3$ = Soller slit, D = semiconductor detector.

ton Gamma Tech pure Ge detector. The Si(Li) detector is usable up to about 35 keV whereas there is practically no upper limit for the Ge detector. The pulse-height analysis was performed using a Canberra Model 8100 multichannel analyser with 1024 channels.

## 3. Procedure

The spectrum from the monochromator consists of several lines, namely the fundamental 111 reflexion and its higher harmonics *. The lines can be shifted on the energy scale by changing the scattering angle, $2\theta_0$.

Most of the observed diffraction lines were used to give a measure of the attenuation for the corresponding energies. The total attenuation coefficient, $\mu$, was obtained from the net counts in each diffraction peak using the formula

$$\mu(E) = t^{-1} \ln [(N_0 - B_0)/(N - B)], \qquad (1)$$

where $t$ is the absorber thickness, $N$ and $N_0$ the total counts in the peak with and without the absorber in the beam path, $B$ and $B_0$ the corresponding background counts, and $E$ the photon energy associated with the diffraction peak.

Boundaries for peak integration were selected according to Heydorn and Lada [6] in order to obtain the optimum statistical precision. The peak position was defined as the maximum of a 4-degree polynomial fitted by the method of least squares to the experimental net counts using orthogonal polynomials [7, 8]. Absorber thickness and the division of counting time between the measurements of $N$ and $N_0$ were optimized according to Nordfors [9].

Each absorption measurement was repeated several times. The mean value of $\mu$ was calculated in such a way as to compensate for any drift in the stabilization of the X-ray generator.

## 4. Errors

The most serious error in the low-energy range is due to the uncertainty in the absorber thickness. In this work the thickness was determined to within 3 $\mu$m, including the uncertainty in placing the absorber perpendicular to the beam.

The error due to counting statistics was minimized using the optimum conditions for absorber thickness, counting times and peak boundary selection as described in the previous section.

The energy determination involves some uncertainties due to the divergence of the collimating system and the channel – to – energy conversion. Finally, small uncontrolled variations in the position of a particular peak during each series of measurements were taken into account.

## 5. Theory

The total attenuation coefficient for X-rays can be written

$$\mu = \begin{cases} \tau + \mu_R + \mu_C, & (2\,a) \\ \tau + \mu_{TDS} + \mu_C, & (2\,b) \end{cases}$$

where $\tau$ is the photoelectric absorption coefficient and $\mu_R$, $\mu_C$ and $\mu_{TDS}$ the contributions due to the coherent or Rayleigh scattering, the incoherent or Compton scattering and the thermal diffuse scattering, respectively.

Equation (2 a) is valid for an isotropic material, whereas (2 b) is valid for a perfect crystal in a position in which no Bragg reflexion occurs.

Formulae for the hydrogen-like photoelectric absorption cross sections have been summarized by Wagenfeld [10]. The calculations are straightforward and fast. This is a great advantage when the absorption has to be known for a large number of photon energies.

The accuracy of the hydrogen-like theory is strongly dependent on the choice of appropriate atomic sub-shell screening constants. In the present work we have used the screening constants determined by Hildebrandt, Stephenson and Wagenfeld [3] from X-ray spin doublet term differences. Recently, Stephenson [11] has published a table of screening constants determined from experimental ionization potentials of spin-paired Pauli-type orbitals. These constants give improved cross sections for incomplete L-shell contributions and are of particular importance for low-$Z$ elements in the soft X-ray region.

In a rigorous treatment the photoelectric absorption cross section is calculated using relativistic wave functions and an appropriate potential to represent the exchange potential experienced by a given electron. Results of such calculations have been published among others by Cromer and Liberman [12] and Storm and Israel [13], to whom the reader is referred for further details. Interpolation of the

* A typical Si hhh diffraction spectrum is shown in Reference 5.

tabulated values has been done on the assumption that $\log\tau$ is proportional to $\log E$.

The scattering cross sections, $\sigma_R$ and $\sigma_C$, due to the Rayleigh scattering and Compton scattering, respectively, are given by [14]

$$\sigma_R = \tfrac{1}{2} r_e^2 \int_{-1}^{1} (1+\cos^2\Phi) f^2(x,Z)\, 2\pi\, \mathrm{d}(\cos\Phi)\ , \quad (3\,\mathrm{a})$$

$$\sigma_C = \tfrac{1}{2} r_e^2 \int_{-1}^{1} [1+k(1-\cos\Phi)]^{-2} \times \{1+\cos^2\Phi + k^2(1-\cos\Phi)^2 \times [1+k(1-\cos\Phi)]^{-1}\} I(x,Z)\, 2\pi\, \mathrm{d}(\cos\Phi)\ , \quad (3\,\mathrm{b})$$

where $r_e$ is the classical electron radius, $k = h\nu/mc^2$ the initial photon energy in electron rest-mass units, $\Phi$ the angle between the incident and scattered photon directions, $x = \sin(\Phi/2)/\lambda$, $Z$ the atomic number, $f(x,Z)$ the atomic scattering factor, and $I(x,Z)$ the incoherent intensity expressed in electronic units.

The table of scattering factors found in the International Tables for X-ray Crystallography Vol. IV [14] was extended by adding those of Hanson, Herman, Lea and Skillman [15] in order to perform the numerical integration for the highest energies. The incoherent scattering intensities used in the calculations were those of Cromer [16] together with the analytical approximations of Balyuzi [17].

The thermal diffuse scattering cross section, $\sigma_{TDS}$, for the approximation of independent vibration of the atoms can be written [18, 19]

$$\sigma_{TDS} = \tfrac{1}{2} r_e^2 \int_{-1}^{1} (1+\cos^2\Phi) f^2(x,Z) \times [1-e^{-2M(x,Z)}]\, 2\pi\, \mathrm{d}(\cos\Phi)\ , \quad (3\,\mathrm{c})$$

where $\exp(-2M)$ is the Debye-Waller factor. Anharmonic effects on the Debye-Waller-factor are assumed to be negligible for silicon and germanium [18].

## 6. Results and Discussion

### 6.1. Silicon

The measured attenuation coefficients are shown in Figure 2. The results for the energy range 25 to 50 keV are listed in Table 1 together with the estimated experimental errors. It is seen that our measurements for energies below 25 keV agree very well with those of Hildebrandt, Stephenson and Wagenfeld [2]. One also notices that the values given in the volume IV of the International Tables for X-ray Crystallography [14] are larger than the experimental values.

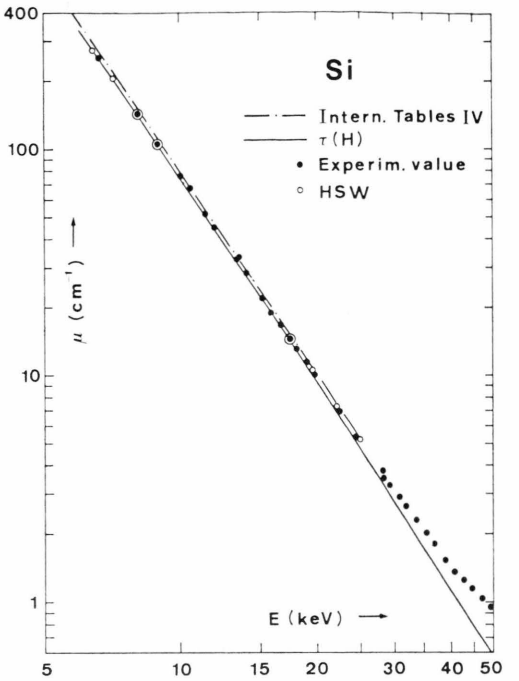


Fig. 2. Total attenuation coefficient of silicon. Filled circles denote our measurements, open circles those of Hildebrandt, Stephenson and Wagenfeld [2]. Comparison with the calculated hydrogen-like photoelectric absorption coefficient (full line) and values from Intern. Tables Vol. IV [14] (broken line).

Table 1. Measured attenuation coefficients of silicon.

| Energy (keV) | $\mu$ (cm$^{-1}$) |
|---|---|
| 24.59 ± 0.04 | 5.2 ± 0.4 |
| 24.60 ± 0.06 | 5.5 ± 0.6 |
| 24.72 ± 0.05 | 5.5 ± 0.3 |
| 28.10 ± 0.05 | 3.8 ± 1.0 |
| 28.26 ± 0.05 | 3.5 ± 0.4 |
| 29.3 ± 0.1 | 3.25 ± 0.01 |
| 30.8 ± 0.2 | 2.90 ± 0.01 |
| 31.7 ± 0.1 | 2.64 ± 0.12 |
| 32.2 ± 0.2 | 2.60 ± 0.01 |
| 33.6 ± 0.2 | 2.29 ± 0.01 |
| 35.3 ± 0.2 | 2.02 ± 0.01 |
| 36.9 ± 0.2 | 1.81 ± 0.01 |
| 39.0 ± 0.2 | 1.53 ± 0.01 |
| 41.1 ± 0.2 | 1.37 ± 0.01 |
| 42.9 ± 0.2 | 1.26 ± 0.01 |
| 44.8 ± 0.2 | 1.14 ± 0.01 |
| 47.1 ± 0.2 | 1.03 ± 0.01 |
| 49.2 ± 0.2 | 0.95 ± 0.01 |

In the energy range 25 to 50 keV the attenuation due to the scattering becomes comparable with the photoelectric absorption. Figure 3 shows the experimental results in this range together with calculations of the total attenuation coefficient.

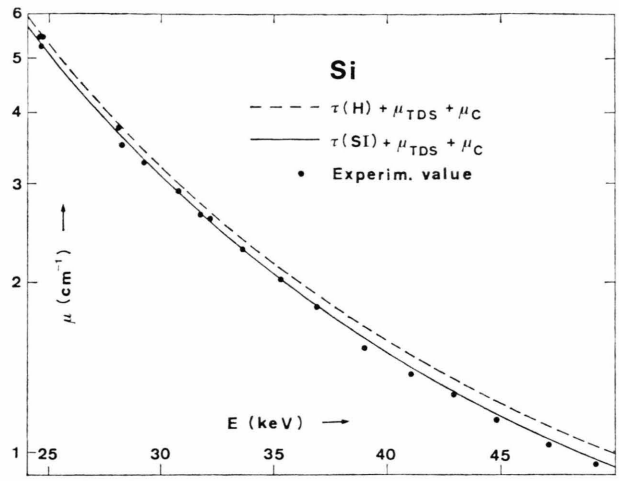


Fig. 3. Total attenuation coefficient of silicon. The measured values (filled circles) are compared with calculated values using the Storm and Israel [13] photoelectric cross sections (full line) and the hydrogen-like theory of photoelectric absorption (broken line) together with thermal diffuse and Compton scattering cross sections.

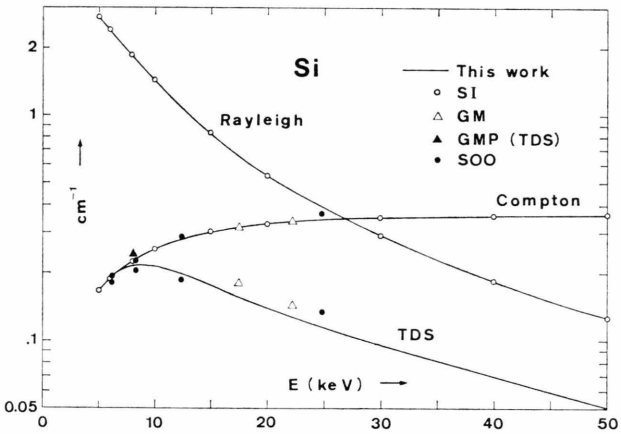


Fig. 4. Scattering attenuation coefficients of silicon. Full lines are calculations of the present work. Comparison with values from Storm and Israel [13] (open circles), Giardina and Merlini [20] (open triangles), Ghezzi, Merlini and Pace [18] (filled triangle, TDS only) and Sano, Ohtaka and Ohtsuki [19] (filled circles).

The scattering attenuation coefficients derived from Eq. (3) are shown as a function of energy in Fig. 4 and compared with calculations of other authors. It is seen that our results fit the available data for the Rayleigh scattering and Compton scattering very well. The results for the thermal diffuse scattering are less conclusive. However, the available data is sparse. Table 2 shows some of the cross sections calculated in the present work for the energy range of interest here. They have been calculated for room temperature using the X-ray Debye temperature $\Theta_M = 532.5$ K. This value was determined for a perfect crystal by Aldred and Hart [21].

Table 2. Calculated thermal diffuse scattering cross sections at room temperature. The values are expressed in units of barns/atom.

| Energy (keV) | Silicon ($\Theta_M$=532.5 K | Germanium ($\Theta_M$=290 K) |
|---|---|---|
| 20 | 2.76 | 27.6 |
| 30 | 1.90 | 19.5 |
| 40 | 1.37 | 13.7 |
| 50 | 1.01 | 10.0 |

The comparison between the theoretical and experimental attenuation coefficients is complicated because different theoretical models have to be used for the photoelectric and scattering processes. Moreover, there is no convenient way of separating the contributions experimentally. Figure 3 indicates, however, that the theoretical photoelectric absorption cross sections of Storm and Israel [13] together with the thermal diffuse scattering and Compton scattering cross sections calculated in the present work form a consistent set of attenuation cross sections. These are in remarkably good agreement with the experimental results. If the photoelectric absorption coefficients from the hydrogen-like theory are used, the total calculated attenuation coefficients are slightly larger than the experimental values as seen in Figure 3.

### 6.2. *Germanium*

Figure 5 and Table 3 summarize the experimental results. Also in this case the agreement with the experimental results of Hildebrandt, Stephenson and Wagenfeld [2] is very good. Figure 5 shows that both the hydrogen-like theory and the tabulation in the volume IV of the International Tables for X-ray Crystallography [14] give a good description of the attenuation in germanium for energies below 25 keV. For energies larger than 30 keV, where the experimental error is smallest, it is obvious that the hydrogen-like theory overestimates the photoelectric absorption. As a matter of fact calculated photoelectric absorption coefficients are larger than the

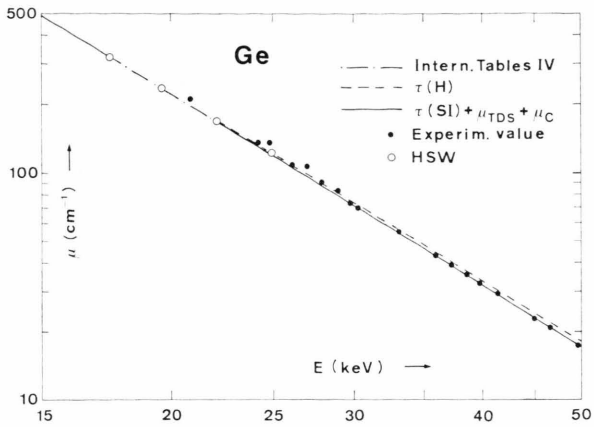


Fig. 5. Total attenuation coefficient of germanium. Filled circles denote our measurements, open circles those of Hildebrandt, Stephenson and Wagenfeld [2]. Comparison with the calculated hydrogen-like photoelectric absorption coefficient (– – –), values from Intern. Tables Vol. IV [14] (—·—) and calculated total attenuation coefficients using the Storm and Israel [13] photoelectric cross sections (———).

Table 3.
Measured attenuation coefficients of germanium.

| Energy (keV) | $\mu$ (cm$^{-1}$) |
|---|---|
| 20.9 ± 0.1 | 212 ± 4 |
| 24.2 ± 0.1 | 137 ± 3 |
| 24.8 ± 0.1 | 136 ± 2 |
| 26.1 ± 0.1 | 108 ± 2 |
| 27.0 ± 0.1 | 107 ± 1 |
| 28.0 ± 0.1 | 91.3 ± 0.6 |
| 29.0 ± 0.1 | 82.9 ± 0.8 |
| 29.8 ± 0.2 | 73.6 ± 0.5 |
| 30.2 ± 0.2 | 69.8 ± 1.4 |
| 33.1 ± 0.2 | 55.4 ± 0.5 |
| 36.0 ± 0.2 | 43.2 ± 0.3 |
| 37.3 ± 0.2 | 39.3 ± 0.2 |
| 38.6 ± 0.2 | 35.8 ± 0.3 |
| 39.7 ± 0.2 | 32.6 ± 0.2 |
| 41.4 ± 0.2 | 29.3 ± 0.3 |
| 45.0 ± 0.2 | 22.7 ± 0.2 |
| 46.6 ± 0.2 | 20.6 ± 0.1 |
| 46.6 ± 0.2 | 20.7 ± 0.1 |
| 49.6 ± 0.2 | 17.0 ± 0.1 |

measured total attenuation coefficients, leaving no room for the scattering contributions.

The scattering cross sections derived from Eq. (3) are shown in Fig. 6 and compared with data from the literature. It is seen that our results fit the data for the Rayleigh scattering and Compton scattering taken from the tables of Storm and Israel [13]. Sano, Ohtaka and Ohtsuki [19] give somewhat larger values for the Compton scattering. Also in this case the available data for the thermal diffuse scattering is sparse. Table 2 shows some of the cross sections calculated in the present work. The X-ray Debye temperature has been assumed to be $\Theta_M = 290$ K, as determined by Ludewig and other authors [22].

Finally, it is seen in Fig. 5 that the total attenuation coefficients derived from Eq. (2 b) using the theoretical photoelectric absorption data of Storm and Israel [13] and the scattering cross sections calculated in the present work are in good agreement with the experimental results. Figure 5 shows that this is true in the whole energy range from 15 to 50 keV considered here.

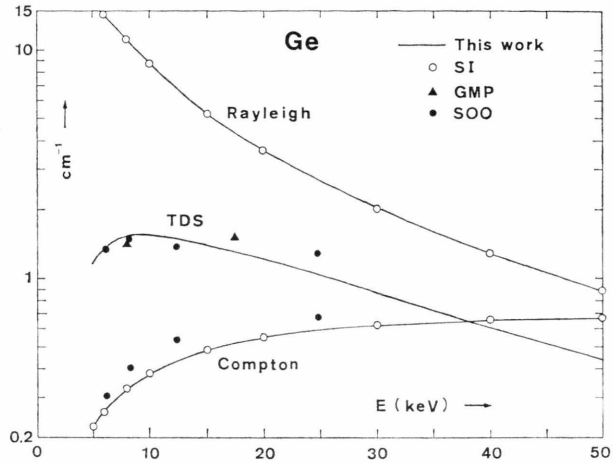


Fig. 6. Scattering attenuation coefficients of germanium. Full lines are calculations of the present work. Comparison with values from Storm and Israel [13] (open circles), Ghezzi, Merlini and Pace [18] (filled triangles) and Sano, Ohtaka and Ohtsuki [19] (filled circles).

## 7. Conclusions

We have measured X-ray attenuation coefficients with a precision between 0.2 and 2% using a continuous X-ray spectrum and energy-dispersive analysis. With a standard X-ray diffraction tube the energy range up to 50 or 60 keV can be covered without changing the tube. Using synchrotron radiation the maximum energy can be still higher.

We have shown that the hydrogen-like theory slightly over-estimates the photoelectric absorption, particularly for germanium in the energy range above 30 keV. The theoretical attenuation coefficients derived from the photoelectric cross sections of Storm and Israel [13] and the cross sections of the thermal diffuse scattering and Compton scattering calculated in the present work are in good agreement with the experimental results for both silicon and germanium single crystals in the whole energy range considered here.

*Acknowledgements*

Financial support from the Danish Natural Science Research Council is gratefully acknowledged. The authors wish to thank Prof. B. Buras for helpful discussions and for putting the Ge detector at our disposal.

[1] H. Hönl, Ann. Physik **18,** 625 [1933]; Z. Physik **84,** 1 [1933].
[2] G. Hildebrandt, J. D. Stephenson, and H. Wagenfeld, Z. Naturforsch. **28 a,** 588 [1973].
[3] G. Hildebrandt, J. D. Stephenson, and H. Wagenfeld, Z. Naturforsch. **30 a,** 697 [1975].
[4] J. D. Stephenson, Z. Naturforsch. **30 a,** 1133 [1975].
[5] B. Buras, J. Staun Olsen, L. Gerward, B. Selsmark, and A. Lindegaard-Andersen, Acta Cryst. **A 31,** 327 [1975].
[6] K. Heydorn and W. Lada, Anal. Chem. **44,** 2313 [1972].
[7] G. B. Forsythe, J. Soc. Indust. Appl. Math. **5,** 74 [1957].
[8] J. S. Thomson and F. Y. Yap, J. Res. Nat. Bur. Std. **72 A,** 187 [1968].
[9] B. Nordfors, Ark. Fys. **18,** 37 [1960].
[10] H. Wagenfeld, Phys. Rev. **144,** 216 [1966].
[11] J. D. Stephenson, Z. Naturforsch. **31 a,** 887 [1976].
[12] D. T. Cromer and D. Liberman, J. Chem. Phys. **53,** 1891 [1970].
[13] E. Storm and H. I. Israel, Nuclear Data Tables **A 7,** 565 [1970].
[14] International Tables for X-Ray Crystallography, Vol. IV, Birmingham 1974.
[15] H. P. Hanson, F. Herman, J. D. Lea, and S. Skillman, Acta Cryst. **17,** 1040 [1964].
[16] D. T. Cromer, J. Chem. Phys. **50,** 4857 [1969].
[17] H. H. M. Balyuzi, Acta Cryst. **A 31,** 600 [1975].
[18] C. Ghezzi, A. Merlini, and S. Pace, Phys. Rev. B **4,** 1833 [1971].
[19] H. Sano, K. Ohtaka, and Y.-H. Ohtsuki, J. Phys. Soc. Japan **27,** 1254 [1969].
[20] M. D. Giardina and A. Merlini, Z. Naturforsch. **28 a,** 1360 [1973].
[21] P. J. E. Aldred and M. Hart, Proc. Roy. Soc. London A **332,** 239 [1973].
[22] J. Ludewig, Acta Cryst. **A 25,** 116 [1969].